

Structural evidence for consecutive Hel308-like modules in the spliceosomal ATPase Brr2

Lingdi Zhang¹, Tao Xu¹, Corina Maeder², Laura-Oana Bud³, James Shanks¹, Jay Nix⁴, Christine Guthrie², Jeffrey A Pleiss³ & Rui Zhao¹

Brr2 is a DExD/H-box helicase responsible for U4/U6 unwinding during spliceosomal activation. Brr2 contains two helicase-like domains, each of which is followed by a Sec63 domain with unknown function. We determined the crystal structure of the second Sec63 domain, which unexpectedly resembles domains 4 and 5 of DNA helicase Hel308. This, together with sequence similarities between Brr2's helicase-like domains and domains 1–3 of Hel308, led us to hypothesize that Brr2 contains two consecutive Hel308-like modules (Hel308-I and Hel308-II). Our structural model and mutagenesis data suggest that Brr2 shares a similar helicase mechanism with Hel308. We demonstrate that Hel308-II interacts with Prp8 and Snu114 *in vitro* and *in vivo*. We further find that the C-terminal region of Prp8 (Prp8-CTR) facilitates the binding of the Brr2–Prp8-CTR complex to U4/U6. Our results have important implications for the mechanism and regulation of Brr2's activity in splicing.

Pre-mRNA splicing is carried out by the spliceosome, which contains five small nuclear RNAs (snRNAs U1, U2, U4, U5 and U6) and more than 100 different proteins. The spliceosome typically assembles on pre-mRNA in a stepwise manner¹. In the first step of spliceosomal assembly, the 5' splice site is recognized by U1 snRNP, the branch point sequence by BBP (SF1 in mammals) and the polypyrimidine tract by MUD2 (U2AF⁶⁵ in mammals). Subsequently, U2 snRNP joins the spliceosome, followed by the joining of the U4/U6–U5 tri-snRNP. Extensive structural rearrangements occur at this stage². For example, base pairing between the 5' splice site and U1 snRNA is disrupted, and the 5' splice site interacts with U6 instead. The base pairing between U4 and U6 is also disrupted and new interactions between U2 and U6 are formed. These rearrangements help to convert the spliceosome to the catalytically active complex, which subsequently splices out the intron and ligates the two exons.

At least eight DExD/H-box proteins are involved at various stage of the splicing cycle³. DExD/H-box proteins include many RNA helicases and belong to helicase superfamily 2 (SF2). All superfamily 1 (SF1) and SF2 helicases contain the minimal helicase domain (two RecA domains with ~400 amino acids encompassing at least eight conserved helicase motifs) and some contain additional domains^{4,5}. Motifs I and II are highly conserved among all SF1 and SF2 helicases, but other motifs are less so, and these are often used to classify SF1 or SF2 helicases into smaller families. DExD/H-box proteins can be further divided into the DEAD, DEAH and Ski2-like DEXH families, as well as a few others⁴. Multiple DExD/H-box proteins in the spliceosome have been demonstrated to have weak helicase activity

in vitro^{6–10}. Although their precise molecular targets remain largely unknown, the DExD/H-box proteins are thought to facilitate the many conformational rearrangements required for the successful assembly and activation of the spliceosome³.

Brr2 is a large DExD/H-box protein (2,163 amino acids in yeast) and a stable component of the U5 snRNP^{7,11,12}. Early experiments identified a role for Brr2 in the unwinding of U4/U6, a crucial step in spliceosomal activation^{7,11,12}. Recent work supports a role for Brr2 in unwinding of U2/U6 during spliceosomal disassembly¹³. As an integral component of the U5 snRNP, tri-snRNP and spliceosome¹⁴, regulation of Brr2's helicase activity is particularly important to ensure the correct timing of spliceosomal activation or disassembly. Prp8 and Snu114 (both components of the U5 snRNP, tri-snRNP and spliceosome) have been implicated in regulating the activity of Brr2 (refs. 2,13,15–17). For example, Brr2's *in vitro* ATPase and helicase activities are modulated by the C-terminal region of Prp8, although the site of modulation on Brr2 and the mechanism of modulation are not known¹⁸.

To our knowledge, Brr2 is one of the only two DExD/H-box proteins (together with Slh1 (ref. 19)) that contain two putative helicase domains, with the second helicase-like domain deviating more from the prototypical helicase motifs^{14,20,21}. Whereas the motifs in the first helicase-like domain of *Saccharomyces cerevisiae* Brr2 have been shown to be crucial for ATPase activity, U4/U6 unwinding and cell viability^{11,12}, the motifs in the second helicase domain can be disrupted with little consequence¹². Brr2 also contains several other domains, including an N-terminal domain and two Sec63 domains. The five domains are

¹Department of Biochemistry and Molecular Genetics, University of Colorado Denver, Aurora, Colorado, USA. ²Department of Biochemistry and Biophysics, University of California, San Francisco, California, USA. ³Department of Molecular Biology and Genetics, Cornell University, Ithaca, New York, USA. ⁴Molecular Biology Consortium, Advanced Light Source, Lawrence Berkeley National Laboratory, Berkeley, California, USA. Correspondence should be addressed to R.Z. (rui.zhao@ucdenver.edu).

Received 17 February; accepted 22 May; published online 14 June 2009; doi:10.1038/nsmb.1625

Table 1 Data collection, phasing and refinement statistics

		Brr2 S2 ^a		
Data collection		<i>P</i> ₂ <i>1</i> ₂ <i>1</i> ₂ <i>1</i>		
Space group				
Cell dimensions				
<i>a</i> , <i>b</i> , <i>c</i> (Å)		55.15, 75.68, 83.96		
		<i>Peak</i>	<i>Inflection</i>	<i>Remote</i>
Wavelength (Å)		0.979	0.9789	0.964
Resolution (Å)	40–2.0 (2.07–2.00) ^b	40–2.0 (2.07–2.00)	40–2.0 (2.07–2.00)	40–2.0 (2.07–2.00)
<i>R</i> _{sym} or <i>R</i> _{merge}	0.084 (0.414)	0.076 (0.422)	0.082 (0.494)	0.082 (0.494)
<i>I</i> / σ <i>I</i>	10.7 (3.9)	12.0 (3.9)	10.3 (2.9)	10.3 (2.9)
Completeness (%)	100.0 (100.0)	100.0 (100.0)	100.0 (100.0)	100.0 (100.0)
Redundancy	7.2 (7.3)	7.2 (7.1)	7.2 (7.1)	7.2 (7.1)
Refinement				
Resolution (Å)	30–2.0			
No. reflections	45,120			
<i>R</i> _{work} / <i>R</i> _{free}	0.246/0.257			
No. atoms				
Protein	2,482			
Water	192			
<i>B</i> -factors				
Protein	36.28			
Water	36.27			
r.m.s. deviations				
Bond lengths (Å)	0.008			
Bond angles (°)	1.674			

^aOne crystal was used for data collection at all three wavelengths. ^bValues in parentheses are for highest-resolution shell.

arranged as shown in **Figure 1a** and are abbreviated as N, H1, S1, H2 and S2. The Sec63 domain is defined by sequence similarity with the Sec63 protein, a central component of the protein-translocation apparatus on the endoplasmic reticulum membrane, although the structure and function of the Sec63 domain are unknown²². With the exception of the H1 domain, which is probably involved in RNA unwinding, the function of the other Brr2 domains is unclear.

We have determined the crystal structure of S2 of *S. cerevisiae* Brr2 and find unexpected structural similarity between S2 and domains 4 and 5 of Hel308 (a Ski2-type SF2 DNA helicase implicated in DNA repair and recombination). This structural similarity, in combination with sequence analyses, led us to hypothesize that the entire Brr2 protein is composed of an N-terminal domain and two consecutive Hel308-like modules. This model offers the first indication of the overall three-dimensional structure of this large and unique spliceosomal ATPase and helicase. The structural similarity with Hel308 suggests mechanistic similarities between Brr2 and Hel308, consistent with mutagenesis data. We also demonstrate that the second Hel308-like module interacts with Prp8 and Snu114 *in vitro* and *in vivo*. Furthermore, we show that Prp8-CTR (residues 1822–2395) facilitates the binding of the Brr2–Prp8-CTR complex to U4/U6, and discuss the implications of this result for the activity and regulation of Brr2.

RESULTS

S2 structure suggests two consecutive Hel308 modules in Brr2

We determined the crystal structure of S2 to 2.0-Å resolution (**Table 1**) and found that S2 is composed of three domains, an N-terminal helical domain, a middle helical domain and a C-terminal β -domain with a fibronectin type 3 (Fn3) fold (**Fig. 1b** and **Supplementary Fig. 1**). The overall structure of yeast Brr2 S2 is highly similar

to the human BRR2 S2 domain (PDB 2Q0Z, Northeast Structural Genomics Consortium) (**Fig. 1c**). The r.m.s. deviation of 269 superimposed main chain atoms between the two structures is 1.6 Å, consistent with the sequence similarity between the two S2 domains (**Supplementary Fig. 2**). All of our subsequent discussion will involve the yeast Brr2 S2 structure we determined.

Despite of the lack of obvious sequence similarity, a structural homology search using the Dali server²³ revealed that the two helical domains of S2 have exactly the same topology as domains 4 and 5 of Hel308, a Ski2-type SF2 DNA helicase (PDB 2P6R)^{24,25} (**Fig. 1d**). Hel308 also contains two RecA domains (domains 1 and 2) and another helical domain 3 (86 residues). The H2 regions of Brr2 share sequence similarity with the two RecA domains common to all SF2 helicases including Hel308 (refs. 14,21). In addition, we noticed that there are ~120 residues immediately downstream of the second RecA domain in H2 that are all helical, based on secondary-structure predictions²⁶. Therefore, the H2 region of Brr2 could resemble domains 1–3 of Hel308 in three-dimensional structures, and the H2+S2 region of Brr2 resembles the entire Hel308 with an additional Fn3 domain (**Fig. 1e**).

The S1 domain of Brr2 is likely to form a similar structure to the S2 domain, given their sequence similarities. Secondary-structure predictions of S1 and S2 match well with the actual secondary structures observed in the S2 structure (**Supplementary Fig. 1**), supporting the hypothesis that S1 forms a similar structure to S2. It is also known that the H1 domain has substantial sequence similarity to the Ski2-type helicase domains (higher than that between H2 and these helicases)¹⁴. It is, therefore, highly likely that the H1+S1 region also forms a structure similar to Hel308. Taken together, we propose that the overall structural of Brr2 consists of an N-terminal domain and two consecutive Hel308-like modules (Hel308-I and Hel308-II) (**Fig. 1e**).

Structural model of Hel308-I suggests helicase mechanisms

Previous mutagenesis studies^{11,12} indicate that Hel308-I is likely to serve the unwinding function of Brr2. Hel308-I has the highest sequence conservation among different species, with 35% identity among Brr2 proteins from yeast, humans, *Caenorhabditis elegans*, *Drosophila melanogaster* and *Arabidopsis thaliana* (MULTALIN²⁷, data not shown). By contrast, only 9% of the residues in the N-terminal domain and 18% of the residues in Hel308-II are absolutely conserved. The high degree of sequence conservation in Hel308-I is probably a reflection of the crucial importance of the helicase activity of this module.

A model of Brr2 Hel308-I can be built based on the crystal structure of Hel308 in complex with a partially unwound DNA duplex (15-bp double-stranded DNA with a 10-nt 3' overhang)²⁴ (**Fig. 1e**). The proposed unwinding mechanism of Hel308 is substantially different from many well-studied DEAD-box RNA helicases. A prominent β -hairpin between motifs V and VI in domain 2 of Hel308 disrupts 2 bp of the double stranded DNA (**Supplementary Fig. 3a**) and is thought to be important for strand separation²⁴. DEAD-box RNA

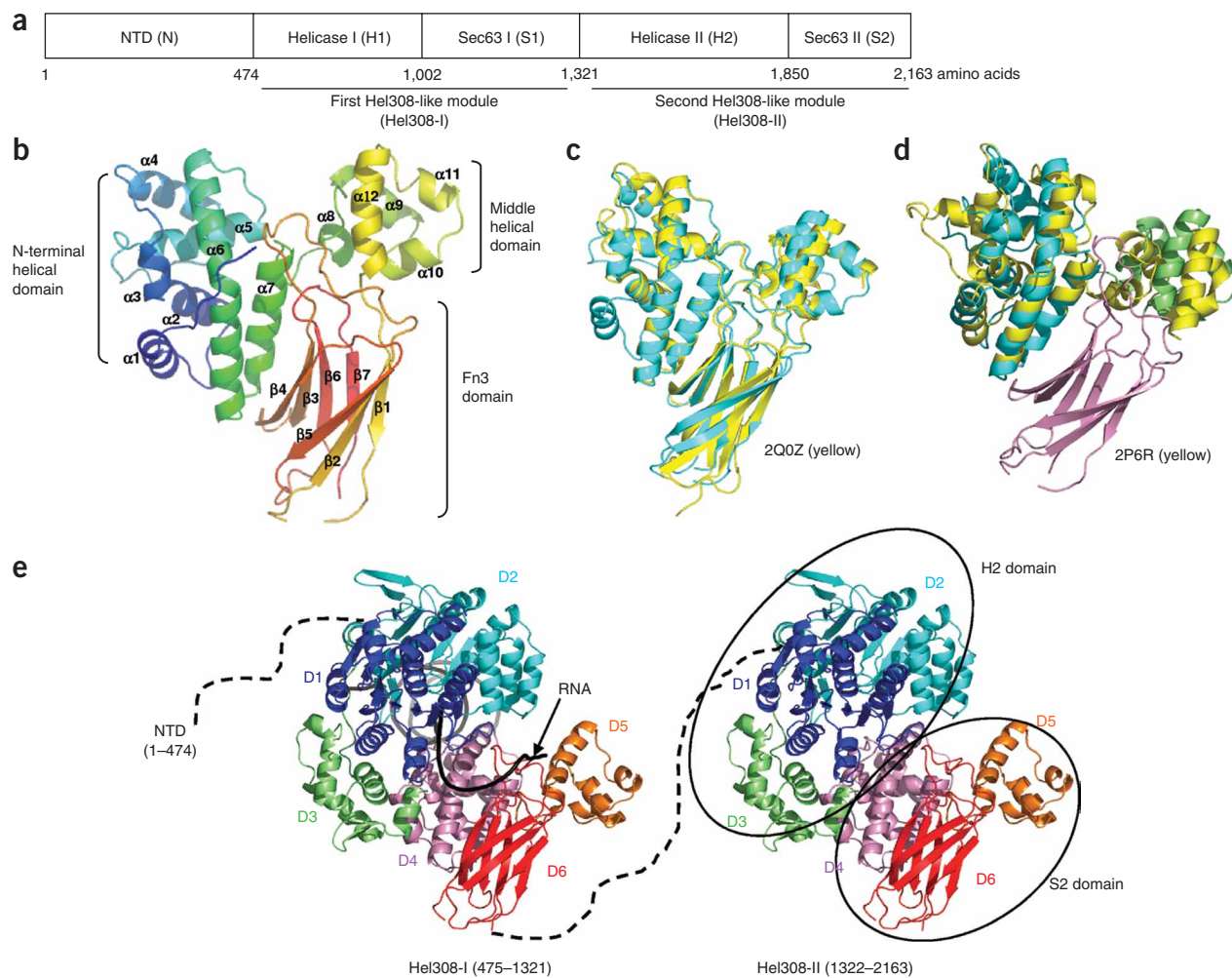


Figure 1 The structure of yeast Brr2. **(a)** A schematic representation of the domain organization (abbreviations shown in parenthesis) of yeast Brr2. **(b)** Overall structure of the S2 domain in rainbow spectrum from the N terminus (blue) to the C terminus (red). **(c)** Superimposition of the yeast (cyan) and human (yellow, PDB 2Q0Z) S2 domain structures. **(d)** Superimposition of the S2 domain and domains 4 and 5 of Hel308 (yellow, PDB 2P6R²⁴). The N-terminal helical domain, the middle helical domain and the C-terminal Fn3 domain in S2 are colored blue, green and purple, respectively. **(e)** A backbone model (by combining the Hel308 and S2 structure) depicting the overall structure of Brr2, including the N-terminal domain (NTD), Hel308-I and Hel308-II. In each Hel308-like module, domains D1–6 are colored in dark blue, light blue, green, purple, orange and red, respectively. A partially unwound DNA duplex (black), as seen in the Hel308 structure, was modeled in Hel308-I to represent the RNA substrate. The traditional H2 and S2 domain are indicated in ovals.

helicases such as eIF4A²⁸, UAP56 (refs. 29,30) and Vasa³¹ do not have a similar β -hairpin and use local RNA bending as an alternative unwinding mechanism³¹. Sequence alignment shows that motifs V and VI of Brr2 are similar to those of Hel308 but are markedly different from the corresponding regions of eIF4A (**Supplementary Fig. 3b**). Brr2 Hel308-I contains a similar number of residues between motifs V and VI as in Hel308 (**Supplementary Fig. 3b**), so it is feasible that Hel308-I also forms a similar β -hairpin in this region, although it is often difficult to accurately predict a short β -hairpin based on secondary-structure predictions. The sequence between motifs V and VI in Brr2 and Hel308 are not well conserved, but this fact does not necessarily conflict with the potential functional importance of this region, as many different amino acid compositions can form a β -hairpin.

As a first step toward exploring the functional importance of the putative β -hairpin region, we generated a *brr2*-3GS mutant by replacing residues 860–865 (WEQLSP, downstream of an existing Gly-Ser pair) with three additional sets of Gly-Ser (**Supplementary Fig. 3b**). Gly-Ser residues have often been used to create flexible linkers in

protein engineering³². We reason that this stretch of four Gly-Ser residues would be likely to disrupt any potential β -hairpin structure in this region, although we realized that the 3GS mutation could potentially be too drastic and disrupt the overall structure of Brr2. We generated *brr2*-3GS on the pGPD-BRR2-TAP vector (containing a C-terminal Protein A tag) and shuffled it into the yTB105 strain (in which endogenous *Brr2* is deleted and wild-type *Brr2* is present on an *URA3*-marked plasmid)¹⁸. The *brr2*-3GS strain grew much more slowly than the wild type at 30 °C and 18 °C and did not grow at 37 °C (**Supplementary Fig. 3c**).

We showed that the Brr2 protein levels in the wild-type and *brr2*-3GS strains were similar by pulling down Brr2 proteins from cell extracts using IgG resin, followed by western blot analyses using an anti-Brr2 antibody³³ (**Supplementary Fig. 3c**). We also demonstrated that Brr2-3GS pulls down similar amounts of Prp8 and Snu114 as wild-type Brr2 (**Supplementary Fig. 3c**), suggesting that the 3GS mutant does not cause major disruption of the overall structure of Brr2. We then purified wild-type Brr2 and Brr2-3GS proteins using

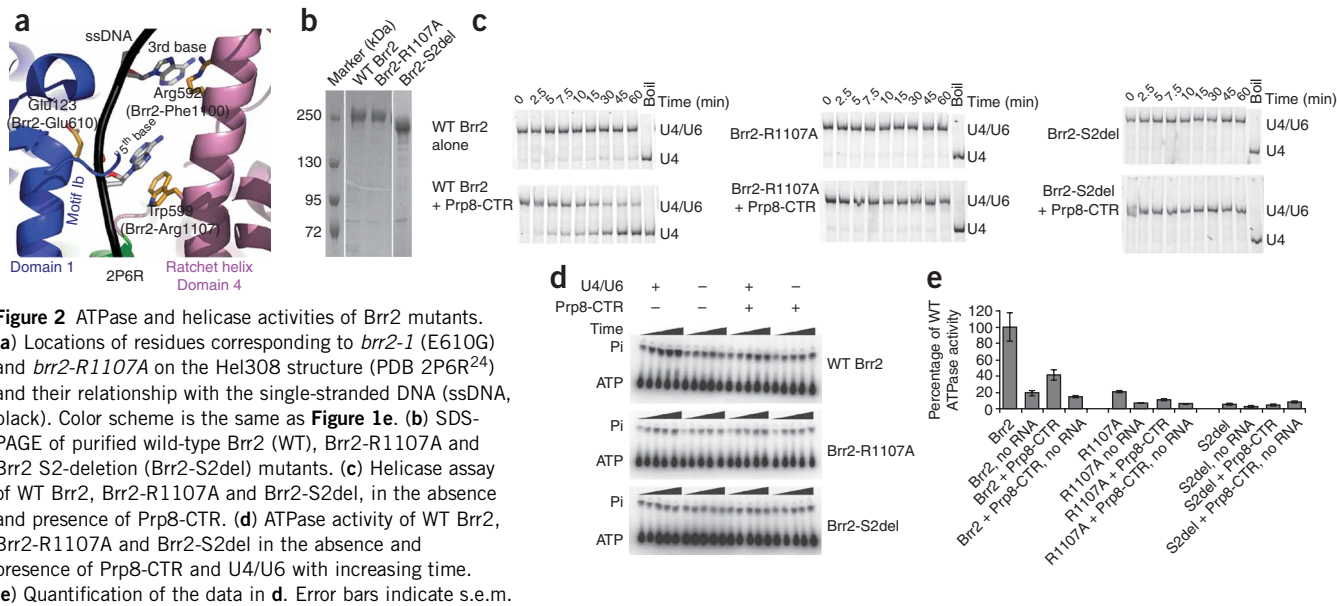


Figure 2 ATPase and helicase activities of Brr2 mutants. **(a)** Locations of residues corresponding to *brr2-1* (E610G) and *brr2-R1107A* on the Hel308 structure (PDB 2P6R²⁴) and their relationship with the single-stranded DNA (ssDNA, black). Color scheme is the same as **Figure 1e**. **(b)** SDS-PAGE of purified wild-type Brr2 (WT), Brr2-R1107A and Brr2 S2-deletion (Brr2-S2del) mutants. **(c)** Helicase assay of WT Brr2, Brr2-R1107A and Brr2-S2del, in the absence and presence of Prp8-CTR. **(d)** ATPase activity of WT Brr2, Brr2-R1107A and Brr2-S2del in the absence and presence of Prp8-CTR and U4/U6 with increasing time. **(e)** Quantification of the data in **d**. Error bars indicate s.e.m.

IgG resin and cleaved off the Protein A tag with TEV protease. As we purified away Brr2-associated proteins, Brr2-3GS became more prone to degradation, so that we obtained less full-length Brr2-3GS protein than wild-type Brr2 (~20% of the wild-type level) (**Supplementary Fig. 3d**). The full-length Brr2-3GS no longer had *in vitro* ATPase and helicase activity¹⁸ (data not shown). Although the loss of helicase activity could be a combination of the effect of the putative β -hairpin itself and other structural changes caused by the 3GS mutation (noting that Brr2-3GS is more prone to degradation in purification and also lost ATPase activity), these results do suggest that the putative β -hairpin region is important for the structure and/or function of Brr2. Further structural, mutagenesis (for example, scanning single-site mutants in the putative β -hairpin region) and biochemical analyses will unambiguously reveal whether Brr2 contains a β -hairpin and uses an unwinding mechanism similar to that of Hel308.

Hel308 is also a relatively processive DNA helicase, in contrast with typical DExD/H-box RNA helicases. In the Hel308–DNA structure, the single-stranded DNA goes through the enclosure formed by domains 1,

3 and 4 and also interacts with domains 2 and 5 (ref. 24). It was suggested that the presence of domains 3 and 4, as well as a central ratchet helix in domain 4, contribute to the processivity of Hel308. Our structural model suggests that similar domains and the ratchet helix also exist in Hel308-I of Brr2, suggesting Brr2 may be more processive than other typical DExD/H-box proteins involved in splicing.

Two previously identified *brr2* mutants are located in the Hel308-I module. *Brr2-1* (E610G) and *Brr2-R1107A* are cold-sensitive (*cs*) mutants that are defective in U4/U6 unwinding¹¹ and/or spliceosome disassembly¹³. Residue Glu610 is located in motif Ib (TPEK in Brr2) of domain 1, which is typically involved in RNA or DNA substrate binding^{24,31}. The equivalent Glu123 residue of Hel308 is indeed present on a helix, right next to the single-stranded DNA in the Hel308–DNA structure²⁴ (**Fig. 2a**). Notably, Hel308-Trp599 (the equivalent of Brr2-Arg1107, **Supplementary Fig. 1**) is present on the midpoint of the ratchet helix of domain 4, across from motif 1b (Brr2-Glu610) on the opposite side of the same single-stranded DNA (**Fig. 2a**). Hel308-Trp599 forms a stacking interaction with the fifth base of the single-stranded DNA. Two helical turns away, Hel308-Arg592 on the same

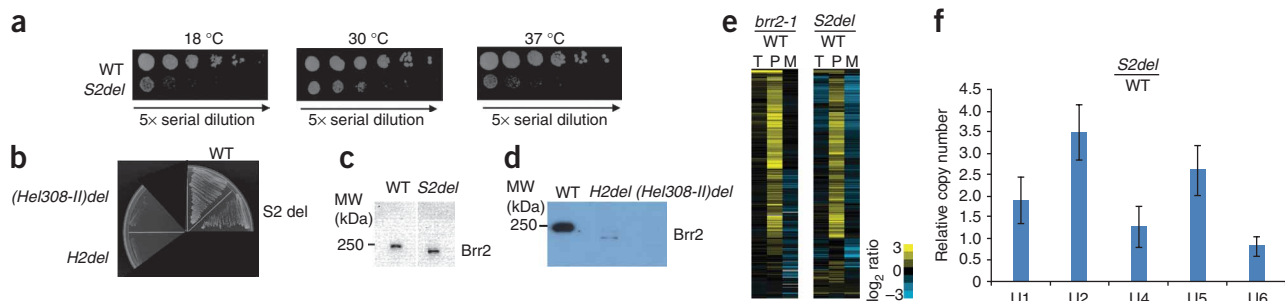


Figure 3 Deletions of domains in Hel308-II lead to growth and splicing defects. **(a)** The S2-deletion mutant (S2del) grows more slowly than the wild-type (WT) *Brr2* strain in all three temperatures. Five fold serial dilutions were plated on YEPD plates and grown at 30 °C and 37 °C for 2 d and at 18 °C for 5 d. **(b)** A 5-FOA plate demonstrating that the S2del strain is viable, but the H2 and Hel308-II deletions are lethal. **(c)** Pull-down experiments using yeast extract and an anti-polyoma antibody, followed by western analyses using an anti-Brr2 antibody, showed that the cellular Brr2 protein levels are similar in the WT and S2del strains. **(d)** Similar pull-down experiments using strains before 5-FOA shuffling showed that the H2 or Hel308-II deletions led to markedly reduced Brr2 protein levels. **(e)** Microarray and quantitative RT-PCR analyses of the genome-wide splicing phenotype and snRNA levels of the S2del strain. Each horizontal line describes the behavior of a single intron-containing gene. 'T', 'P' and 'M' represent total mRNA, pre-mRNA and mature mRNA, respectively. Yellow indicates increased and blue indicates decreased RNA levels compared to the WT. **(f)** Total snRNA levels assessed using quantitative RT-PCR indicates that the S2del mutation leads to an accumulation of the U1, U2 and U5 snRNAs. Error bars indicate s.d.

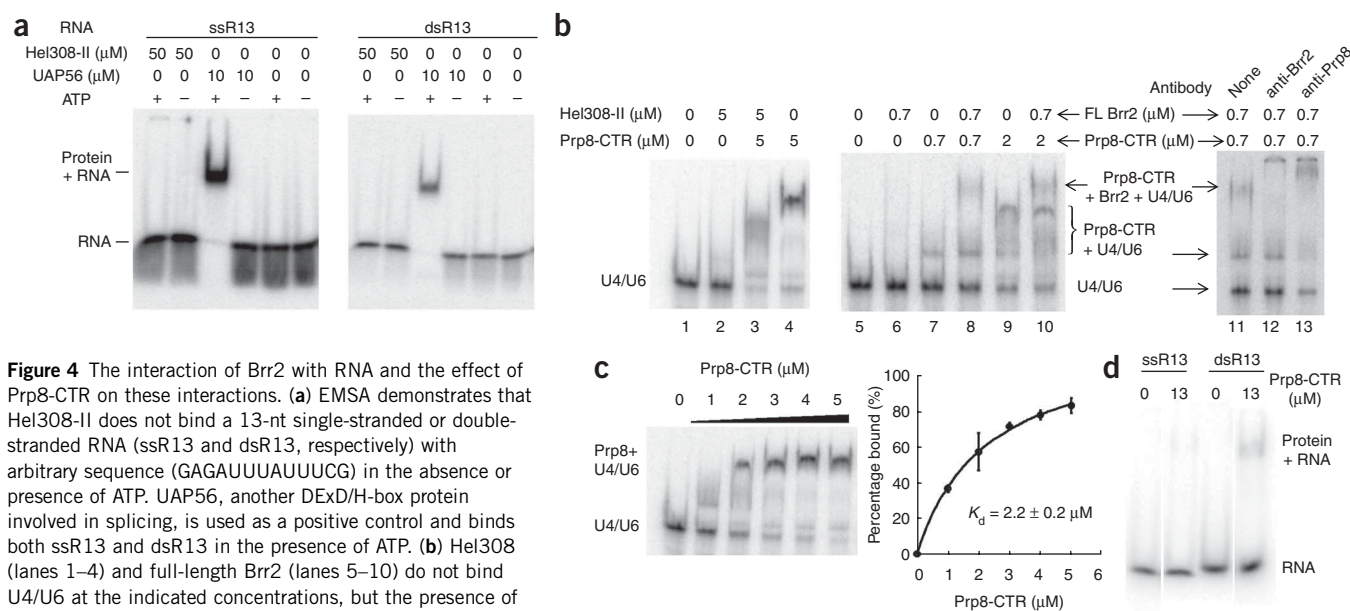


Figure 4 The interaction of Brr2 with RNA and the effect of Prp8-CTR on these interactions. **(a)** EMSA demonstrates that Hel308-II does not bind a 13-nt single-stranded or double-stranded RNA (ssR13 and dsR13, respectively) with arbitrary sequence (GAGAUUUUUUUCG) in the absence or presence of ATP. UAP56, another DExD/H-box protein involved in splicing, is used as a positive control and binds both ssR13 and dsR13 in the presence of ATP. **(b)** Hel308 (lanes 1–4) and full-length Brr2 (lanes 5–10) do not bind U4/U6 at the indicated concentrations, but the presence of Prp8-CTR generates a complex that binds U4/U6 more efficiently. Supershift experiments using anti-Brr2 and anti-Prp8 antibodies confirm the identity of the shifted bands (lanes 11–13). **(c)** Titration experiments indicate that Prp8-CTR binds U4/U6 with a K_d of $2.2 \pm 0.2 \mu\text{M}$. Error bars and errors in K_d are s.d. **(d)** Prp8-CTR binds ssR13 or dsR13 weakly.

helix interacts with the third base of the single-stranded DNA. In addition, the N terminus of the ratchet helix interacts with motif IVa of domain 2. Therefore, ATP-dependent movement of domain 2 was thought to modulate the position of the ratchet helix and facilitate strand translocation²⁴. Brr2-Phe1100 (the equivalent of Hel308-Arg592) in combination with Brr2-Arg1107 (the equivalent of Hel308-Trp599) can potentially perform a similar function to Hel308-Arg592 and Hel308-Trp599 in strand translocation and processivity. Mutations of Brr2-Glu610 (that is, *brr2-1*) and Brr2-Arg1107 (that is, *brr2-R1107A*) may conceivably affect RNA binding and/or strand translocation and, consequently, affect U4/U6 unwinding and spliceosomal disassembly. Indeed, Brr2-1 does not have detectable unwinding activity in an *in vitro* helicase assay¹⁸.

To test the role for Arg1107 in Brr2 function, we constructed the R1107A mutant on the pGPD-BRR2-TAP vector and shuffled the mutant plasmid into the yTB105 strain. We were able to purify a similar quantity of Brr2-R1107A and wild-type Brr2 (**Fig. 2b**) for ATPase and helicase assays. As previously observed¹⁸, wild-type Brr2 demonstrates weak helicase activity on its own, but the activity is greatly stimulated by Prp8-CTR (the previously used Prp8 region consists of residues 1806–2413 and is highly similar to our Prp8-CTR, which consists of residues 1822–2395) (**Fig. 2c**). Wild-type Brr2 also showed RNA-stimulated ATPase activity, which could be inhibited by Prp8-CTR (**Fig. 2d,e**). The Brr2-R1107A mutant had greatly reduced ATPase activity and no detectable helicase activity under the present assay conditions (**Fig. 2c–e**). Both Brr2-1 and Brr2-R1107A probably retain weak helicase activity *in vivo*, because yeast strains containing these mutants grew similarly to the wild-type strain at 30 °C. In general, these results support the mechanistic similarity between Brr2 and Hel308.

Domain deletions in Hel308-II are lethal or detrimental to growth

In contrast to the likely unwinding function of Hel308-I, the Hel308-II module of Brr2 does not have ATPase activity and is unlikely to have helicase activity¹². We focused our subsequent studies on

understanding the function of Hel308-II. We generated yeast strains carrying Brr2 with the H2, S2 or Hel308-II (H2+S2) domains deleted. These deletions were constructed on pPR150 (carrying a C-terminal polyoma tag)¹¹ and were shuffled into yeast strain yJPS996 (in which endogenous *Brr2* is deleted and wild-type *Brr2* is present on an *URA3*-marked plasmid)¹³. The S2-deletion strain grew much more slowly than the wild-type strain at all three temperatures (**Fig. 3a**). All other deletion strains did not grow on 5-fluoroorotic acid (5-FOA) plates (**Fig. 3b**), indicating that these deletions are lethal. We then performed pull-down experiments using yeast extract and an anti-polyoma antibody, followed by western blotting with an anti-Brr2 antibody³³. There were similar quantities of Brr2 protein in both the wild-type and the S2-deletion strains (**Fig. 3c**), indicating that the slow-growth phenotype of the S2-deletion was not caused by the lack of Brr2 protein. We also performed similar pull-down experiments using yeast strains before 5-FOA shuffling. The H2 and Hel308-II deletion strains contained much less Brr2 protein than the wild-type strain, indicating that these deletions destabilize the Brr2 protein (**Fig. 3d**).

S2 deletion affects the splicing of many genes

To examine the molecular phenotype of the S2 deletion, we performed splicing-specific microarray experiments. These microarrays contain three probes for each of the ~300 intron-containing genes in yeast: one targeting a region of the intron to measure pre-mRNA levels, one targeting the junction between exons 1 and 2 to measure the mature mRNA and one targeting a region of either exon 1 or 2 to measure changes in total mRNA³⁴. As a control, we simultaneously examined the behavior of the *brr2-1* strain¹¹. The microarray data show that the S2 deletion affects the splicing of the vast majority of intron-containing genes, as demonstrated by the accumulation of pre-mRNA and reduction of spliced mRNA for these genes (**Fig. 3e**). The defects seen in the S2 deletion, in terms of both the number of transcripts whose splicing is affected and the magnitude to which their splicing is affected, are similar in scale to the defects seen in the *brr2-1* strain (**Fig. 3e**), indicating a strong defect in pre-mRNA splicing. Notably, the S2 deletion, but not the *brr2-1* mutation, also showed accumulation

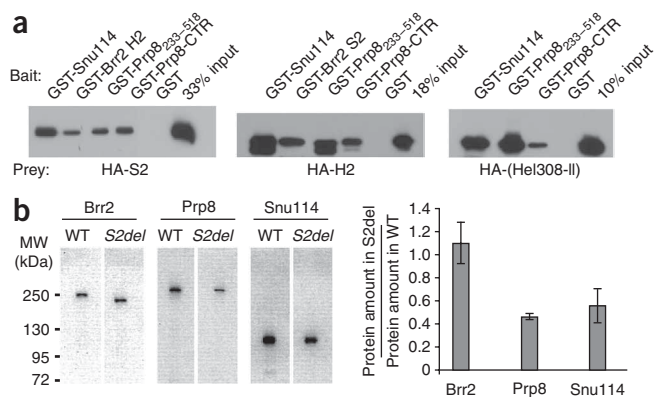


Figure 5 Hel308-II interacts with Prp8 and Snu114 *in vitro* and *in vivo*. (a) GST pull-down experiments demonstrate that the H2, S2 and Hel308-II domains interact with Prp8 and Snu114. HA, hemagglutinin. (b) Co-immunoprecipitation experiments demonstrate that the S2-deletion (S2del) strain has a similar level of Brr2 but a lower level of Prp8 and Snu114 than the wild-type (WT) strain. Brr2 in yeast extract was pulled down using anti-polyoma antibody and probed in a western blot using anti-Brr2, anti-Prp8 and anti-Snu114 antibodies. Error bars indicate s.d.

of U1, U2 and U5 snRNAs (1.9-fold, 3.5-fold and 2.6-fold, respectively) through quantitative RT-PCR analyses (Fig. 3f). The mechanism and significance of this accumulation await further studies.

Hel308-II does not bind several RNAs tested *in vitro*

We next examined whether Hel308-II retains the ability to bind to RNA, even though it lacks ATPase and helicase activities (Fig. 4). We demonstrated using an electrophoresis mobility shift assay (EMSA) that purified Hel308-II does not bind a 13-nt single-stranded or double-stranded RNA (using the arbitrary sequence GAGAUUUUUUCG, designated as ssR13 and dsR13 for the single- and double-stranded forms, respectively), even at a Hel308-II concentration of 50 μ M, in the absence or presence of ATP (Fig. 4a). Under similar conditions, the positive control UAP56 (a splicing factor and DEAD-box protein) clearly binds RNA at a concentration of 10 μ M UAP56 in the presence of ATP (ATP is known to increase the RNA binding affinity of many DEAD-box proteins, including eIF4A^{31,35}) (Fig. 4a). Nor does Hel308-II have detectable binding to U4/U6 at 5 μ M protein concentration in the presence or absence of ATP (Fig. 4b, lanes 1 and 2).

Hel308-II interacts with Prp8 and Snu114 *in vitro*

We then evaluated whether the Hel308-II module can potentially function as a protein-interaction domain and mediate interactions with other spliceosomal proteins. We performed *in vitro* glutathione S-transferase (GST) pull-down experiments using GST-fused versions of several Brr2 domains, Prp8 domains and Snu114 as baits, and hemagglutinin-tagged Brr2 H2, S2 or Hel308-II domains as prey (Fig. 5a). These experiments demonstrate that the H2 and S2 domain of Brr2 interact with each other, consistent with the idea that the H2 and S2 domains come together to form a Hel308 module. Furthermore, the H2, S2 and Hel308-II domains all interact with both the N-terminal (residues 233–518) and C-terminal (Prp8-CTR, residues 1822–2395) regions of Prp8, as well as with Snu114. These interactions are specific, as no interaction is detected with GST alone. Our results are consistent with previous observations using yeast two-hybrid analyses that the C-terminal region of yeast Brr2 (a construct containing the combination of residues 112–356 and 1184–2163) is responsible for the vast majority of interactions between Brr2 and

many spliceosomal proteins including Prp8 (ref. 36). The interactions between the H2 domain of human BRR2 with PRP8 and SNU114 have also been observed previously using yeast two-hybrid analyses^{37,38}.

S2 deletion decreases Brr2's association with Prp8 and Snu114

We took advantage of the fact that the S2-deletion strain is viable to examine whether the S2 domain also interacts with Prp8 and Snu114 *in vivo*. We immunoprecipitated Brr2 from extracts of the wild-type and S2-deletion strains using an anti-polyoma antibody. We then performed western blot analyses on the immunoprecipitated sample using anti-Brr2 (ref. 33), anti-Prp8 (ref. 39) and anti-Snu114 (ref. 40) antibodies. The level of Brr2 protein in the immunoprecipitated sample from the S2-deletion strain was similar to that of the wild-type, but the level of Prp8 and Snu114 was much less in the S2-deletion strain (about 50% of the wild-type level) (Fig. 5b). These experiments demonstrate that S2 deletion is defective in Prp8 and Snu114 binding, suggesting that the S2 domain indeed participates in Prp8 and Snu114 interactions *in vivo*.

S2 deletion reduces the ATPase and helicase activity of Brr2 *in vitro*

To evaluate the effects of the S2 deletion on the ATPase and helicase activity of Brr2, we replaced the wild-type *Brr2* in the pGPD-Brr2-TAP vector¹⁸ with the S2-deleted *brr2*. We expressed the full-length and S2-deleted Brr2 from yeast strain yTB105 (ref. 16), purified proteins using IgG resin and cleaved off the Protein A tag with TEV protease. We obtained similar quantities of purified proteins (Fig. 2b) for ATPase and helicase assays. The S2 deletion reduced Brr2's ATPase and helicase activities to levels that are undetectable in these assays (Fig. 2c–e). The S2-deleted Brr2 is likely to still have weak ATPase and helicase activities *in vivo*, because the S2-deletion strain was viable even though it grew much more slowly than the wild-type strain. These results suggest that the S2 domain and Hel308-I interact, or communicate, with each other, and the S2 domain potentially stabilizes the structure and conformation of Hel308-I. The S2 deletion does not seem to lead to a complete misfolding of Brr2, because the S2-deletion strain was still viable and we were able to purify similar quantities of soluble S2-deleted Brr2 protein as wild-type Brr2 protein (Fig. 2b). However, the S2 deletion probably leads to certain conformational changes in Hel308-I, rendering it less active in ATPase and helicase assays.

Prp8-CTR facilitates binding of Brr2–Prp8-CTR to U4/U6

We then examined the effect of Prp8-CTR on the RNA binding property of Brr2, using both Hel308-II and full-length Brr2. We showed using EMSA that Brr2 Hel308-II at 5 μ M concentration does not bind U4/U6 appreciably (Fig. 4b, lane 2). Prp8-CTR, on the other hand, binds and shifts essentially all of the U4/U6, when present at 5 μ M concentration (Fig. 4b, lane 4). We performed a titration experiment and determined that the K_d of Prp8-CTR to U4/U6 is $2.2 \pm 0.2 \mu$ M (Fig. 4c). This affinity is substantially higher than the affinity of Prp8-CTR to ssR13 and dsR13, where 13 μ M Prp8-CTR showed essentially no binding to ssR13 and little binding to dsR13 (Fig. 4d). When Brr2 Hel308-II and Prp8-CTR were incubated together with U4/U6, nearly all of the U4/U6 shifted to a position different from the band formed by Prp8-CTR alone with U4/U6 (Fig. 4b, compare lane 3 with lane 4). We interpreted this new gel-shift band as the Prp8-CTR–Hel308-II–U4/U6 complex (Fig. 4b, lane 3).

Full-length Brr2 at 0.7 μ M did not show appreciable binding to U4/U6 (Fig. 4b, lanes 5 and 6). Addition of 0.7 μ M Prp8-CTR (lane 8) resulted in a band at the same position as the band formed with

Prp8-CTR alone plus U4/U6 (lane 7) and, importantly, a new, slower-migrating band that probably corresponds to the Prp8-CTR-Brr2-U4/U6 complex. Supershift experiments using anti-Prp8 (ref. 39) and anti-Brr2 (ref. 33) antibodies (Fig. 4b, lanes 11–13) confirmed our assignment of the faster-migrating band as Prp8-CTR alone plus U4/U6 and the slower-migrating band as Prp8-CTR-Brr2-U4/U6. The addition of more Prp8-CTR (lane 10) continued to form the band corresponding to the Prp8-CTR alone plus U4/U6 band seen in lane 9, as well as a new band that probably represents the Prp8-CTR-Brr2-U4/U6 complex. Note the positions of the Prp8-CTR alone plus U4/U6 bands are different at 0.7 μ M and 2 μ M Prp8-CTR concentrations (compare lane 7 with lane 9) for reasons we do not fully understand, and this phenomenon was also observed in the K_d -determination experiment in Figure 4c. All binding reactions were highly reproducible and performed both in the absence and presence of ATP, yielding identical results (data not shown). These results indicate that Prp8-CTR can facilitate the binding of the Brr2-Prp8-CTR complex to U4/U6.

DISCUSSION

Our structural studies in combination with sequence analyses suggest that the H2+S2 domain of Brr2 resembles the entire Hel308 and that the full-length Brr2 protein is composed of an N-terminal domain and two consecutive Hel308-like modules (Hel308-I and Hel308-II). A recent structure of another Ski2-type DNA helicase, Hjm, also revealed a similar domain structure and organization as Hel308 (ref. 41). This raises the possibility that many Ski2-type helicases may share structural (and potentially mechanistic) similarities in regions beyond the helicase domains, despite of the lack of recognizable sequence similarities in these regions.

The structural resemblance between Brr2 and Hel308 suggests possible helicase mechanisms for Brr2. Our *brr2-3GS* mutant suggests that the putative β -hairpin region in Brr2 Hel308-I is structurally and/or functionally important. Further structural and mutational analyses will reveal whether Brr2 indeed contains a β -hairpin and uses an unwinding mechanism similar to Hel308 (ref. 31). Furthermore, our structural mapping and biochemical analyses of the *brr2-1* and *brr2-R1107A* mutants support the structural and mechanistic similarity between Brr2 and Hel308. These results suggest the possibility that Brr2 is more processive than other DExD/H-box proteins involved in pre-mRNA splicing. This potential processivity is attractive, considering that yeast Brr2 needs to unwind U4/U6, which contains long stem regions and is highly stable in yeast⁴¹.

Brr2 is one of two known helicases (together with Slh1) that contains two helicase-like modules. The function of the second helicase-like module has long been elusive and intriguing. There are several substantial deviations between the putative helicase motifs in Hel308-II and the canonical helicase motifs. For example, the typical DExD/H residues in motif II are replaced with DDAH in Hel308-II (Supplementary Fig. 4). The glutamate of motif II (DExD/H) has been postulated to be the key catalytic residue that activates a water molecule to hydrolyze ATP in DExD/H-box proteins and other helicases^{5,31,43}. Likewise, the Ser-Ala-Thr (SAT) residues in motif III are replaced with SNC in Hel308-II (Supplementary Fig. 4). The SAT residues in motif III do not interact with ATP or RNA but participate in interdomain interactions between the N-terminal and C-terminal domains upon ATP and RNA binding, and they are thought to be important for the unwinding activity of DExD/H-box proteins³¹. Hel308-II also lacks obvious motifs IV–VI (Supplementary Fig. 4). Substantial deviations from the canonical helicase motifs in Hel308-II have probably led to the lack of ATPase and helicase activities of this module.

We demonstrated that Hel308-II interacts with Prp8 and Snu114 *in vitro* and *in vivo* (Fig. 5). We do not rule out the possibility that Prp8 and Snu114 also interact with the Hel308-I module, although we cannot yet test this hypothesis because Hel308-I alone is unstable. It is worth noting that protein tag labeling and antibody recognition approaches have mapped the C terminus of Brr2 to be somewhat distant from the C terminus of Prp8 in the EM projection structure of the yeast tri-snRNP, whereas the C termini of Prp8 and Snu114 are in close proximity to each other⁴⁴. However, these labeling methods are designed to map the extreme C terminus of a protein. The longest dimension of Hel308 is about 80 Å, and the Prp8-CTR can reach similar dimensions depending on the relative orientation of its C-terminal and β -finger domains^{38,45–48}. This dimension can easily span the distance between the C termini of Brr2 and Prp8 observed in the EM structure⁴⁴. Therefore, the main body of Brr2 Hel308-II and Prp8-CTR can overlap and interact with each other, even if the extreme C termini of Brr2 and Prp8 are far from each other. Our results, in general, represent the first example of a helicase-like structural fold serving as a major protein-interaction platform.

The Hel308-II module could potentially have a role in mediating the regulation of Brr2 activity. Recently, it was shown that the C-terminal fragment of Prp8 (residues 1806–2413) greatly stimulates Brr2's helicase activity but inhibits its ATPase activity *in vitro*¹⁸. Here we show that the deletion of S2 results in a strong reduction of Brr2's ATPase and helicase activity (Fig. 2c–e). We also find that the deletion of Hel308-II markedly destabilizes the protein (Fig. 3d). Both results suggest that the S2 domain, and the entire Hel308-II module, interact and communicate with Hel308-I. It is possible that the interaction between Prp8 and Hel308-II potentially affect the structure and/or stability of Hel308-I and, consequently, the ATPase and helicase activity of Brr2. We do not rule out the possibility that Prp8 may directly interact with Hel308-I to modulate Brr2's activity. Either directly (through Hel308-I) or indirectly (through Hel308-II), Prp8 may affect Brr2's ATPase and helicase activities by increasing its RNA binding affinity, stabilizing a favorable conformational change, increasing processivity or a combination of the above. In analogous situations, detailed kinetics analyses suggest that eIF4B, eIF4H and eIF4G stimulate eIF4A's ATPase and helicase activity through one or more of the above mechanisms⁴⁹. Likewise, Ntr1 was recently shown to stimulate the activity of Prp43 (another DExD/H-box protein involved in spliceosome disassembly) and was thought to affect Prp43's processivity⁵⁰.

Our observation of the effect of Prp8-CTR on Brr2's RNA binding property raises another interesting possibility for the regulation of Brr2's activity. We showed that Prp8-CTR binds U4/U6 with a much higher affinity than it binds to arbitrary 13 nt single-stranded or double-stranded RNAs (Fig. 4c,d). When Prp8-CTR and Brr2 (Hel308-II or full-length protein) are combined, the complex binds U4/U6 much better than Brr2 alone (Fig. 4b). We cannot at this point differentiate whether Prp8-CTR increases Brr2's intrinsic affinity to U4/U6 or the increased binding is solely attributed to Prp8-CTR in the complex. However, in either case, the interaction between Prp8-CTR and Brr2 clearly helps the complex to bind U4/U6 better. This increased affinity provides a possible mechanism for how Prp8-CTR helps Brr2 to confer specificity toward U4/U6. Further studies will reveal the extent of this specificity, such as how stringent the Prp8-CTR is toward the sequence and/or structure of U4/U6. It is worth noting that one study found that the N-terminal RNase H domain of the human PRP8-CTR has a much higher binding affinity with a U2/U6 mimic than with other RNAs⁴⁷, consistent with the possibility that Prp8 may also help Brr2 confer specificity toward U2/U6 to

facilitate Brr2's role in U2/U6 unwinding. The higher local concentration of U4/U6 brought to Brr2 by Prp8-CTR could also serve as an additional mechanism for the stimulation effect by Prp8-CTR that we observed *in vitro*. There are other enzymes (such as collagen prolyl 4-hydroxylase, HIV integrase and endonuclease NaeI) that have separate substrate binding and catalytic domains, especially when the substrate is a polypeptide or oligonucleotide^{51–53}. Prp8 could potentially serve as an auxiliary substrate binding and specificity domain for Brr2.

Our results also lead to reflections on the function of the Sec63 domain in general. Our structural result shows that the so-called Sec63 domain is in fact made of three domains, two helical and one all- β Fn3 domains. The Sec63 domain has at least two functions. It can serve as a major RNA binding and processivity domain, as in the case of Hel308-I. It can also serve as a major protein interaction domain, as in the case of Hel308-II. The Fn3 fold in the Sec63 domain belongs to the immunoglobulin-like superfamily, whose members are almost always involved in binding functions⁵⁴. Deletion of the Sec63 domain in the Sec63 protein leads to impaired higher-order complex formation⁵⁵. This Sec63 domain may also have a role in protein interaction, indicating the generality of the Sec63 domain serving as a protein interaction domain.

METHODS

Methods and any associated references are available in the online version of the paper at <http://www.nature.com/nsmb/>.

Accession codes. Protein Data Bank: the structure of yeast Brr2 S2 is deposited with accession code 3HIB. NCBI Gene Expression Omnibus: the splicing microarray data is deposited with accession code GSE16135.

Note: Supplementary information is available on the Nature Structural & Molecular Biology website.

ACKNOWLEDGMENTS

We are grateful to J. Staley (University of Chicago) and S. Stevens (University of Texas Austin) for providing yeast strains and plasmids; J. Beggs (University of Edinburgh) for anti-Brr2 antibody; and P. Fabrizio (Max Planck Institute for Biophysical Chemistry) for anti-Snu114 antibody. We thank B. Chong for help generating preliminary crystals. We thank the X-ray facility (supported in part by the University of Colorado Cancer Center) at the University of Colorado Denver. R.Z. is supported by a Kimmel Scholar award. C.G. is an American Cancer Society Research Professor of Molecular Genetics. This work was supported by a grant from the US National Institutes of Health (NIH) to R.Z. (GM080334), an American Cancer Society Research Scholar grant to R.Z. (RSG-06-165-01-GMC), a NIH grant to C.G. (GM21119), an American Heart Association postdoctoral fellowship to L.Z. (0820036Z) and a National Institutes of General Medical Sciences postdoctoral fellowship to C.M. (F32GM077844).

AUTHOR CONTRIBUTIONS

L.Z., T.X., C.M., L.-O.B., C.G., J.A.P. and R.Z. designed and analyzed the experiments; L.Z., T.X., C.M., L.-O.B., J.S., J.N., J.A.P. and R.Z. performed the experiments; R.Z. wrote the paper.

Published online at <http://www.nature.com/nsmb/>

Reprints and permissions information is available online at <http://npg.nature.com/reprintsandpermissions/>

- Burge, C.B., Tuschl, T.H. & Sharp, P.A. Splicing of precursors to mRNAs by the spliceosome. in *The RNA World* (eds. Gesteland, R.F., Cech, T. & Atkins, J.F.) 525–560 (Cold Spring Harbor Laboratory Press, Cold Spring Harbor, 1999).
- Brow, D.A. Allosteric cascade of spliceosome activation. *Annu. Rev. Genet.* **36**, 333–360 (2002).
- Staley, J.P. & Guthrie, C. Mechanical devices of the spliceosome: motors, clocks, springs, and things. *Cell* **92**, 315–326 (1998).

- Jankowsky, E. & Fairman, M.E. RNA helicases—one fold for many functions. *Curr. Opin. Struct. Biol.* **17**, 316–324 (2007).
- Cordin, O., Barroques, J., Tanner, N.K. & Linder, P. The DEAD-box protein family of RNA helicases. *Gene* **367**, 17–37 (2006).
- Wagner, J.D., Jankowsky, E., Company, M., Pyle, A.M. & Abelson, J.N. The DEAH-box protein PRP22 is an ATPase that mediates ATP-dependent mRNA release from the spliceosome and unwinds RNA duplexes. *EMBO J.* **17**, 2926–2937 (1998).
- Laggerbauer, B., Achsel, T. & Luhrmann, R. The human U5–200kD DEXH-box protein unwinds U4/U6 RNA duplexes *in vitro*. *Proc. Natl. Acad. Sci. USA* **95**, 4188–4192 (1998).
- Wang, Y., Wagner, J.D. & Guthrie, C. The DEAH-box splicing factor Prp16 unwinds RNA duplexes *in vitro*. *Curr. Biol.* **8**, 441–451 (1998).
- Tanaka, N. & Schwer, B. Mutations in PRP43 that uncouple RNA-dependent NTPase activity and pre-mRNA splicing function. *Biochemistry* **45**, 6510–6521 (2006).
- Shen, J., Zhang, L. & Zhao, R. Biochemical characterization of the ATPase and helicase activity of UAP56, an essential pre-mRNA splicing and mRNA export factor. *J. Biol. Chem.* **282**, 22544–22550 (2007).
- Raghunathan, P.L. & Guthrie, C. RNA unwinding in U4/U6 snRNPs requires ATP hydrolysis and the DEIH-box splicing factor Brr2. *Curr. Biol.* **8**, 847–855 (1998).
- Kim, D.H. & Rossi, J.J. The first ATPase domain of the yeast 246-kDa protein is required for *in vivo* unwinding of the U4/U6 duplex. *RNA* **5**, 959–971 (1999).
- Small, E.C., Leggett, S.R., Winans, A.A. & Staley, J.P. The EF-G-like GTPase Snu114p regulates spliceosome dynamics mediated by Brr2p, a DEX/H box ATPase. *Mol. Cell* **23**, 389–399 (2006).
- Lauber, J. *et al.* The HeLa 200 kDa U5 snRNP-specific protein and its homologue in *Saccharomyces cerevisiae* are members of the DEXH-box protein family of putative RNA helicases. *EMBO J.* **15**, 4001–4015 (1996).
- Grainger, R.J. & Beggs, J.D. Prp8 protein: at the heart of the spliceosome. *RNA* **11**, 533–557 (2005).
- Brenner, T.J. & Guthrie, C. Genetic analysis reveals a role for the C terminus of the *Saccharomyces cerevisiae* GTPase Snu114 during spliceosome activation. *Genetics* **170**, 1063–1080 (2005).
- Bartels, C., Klatt, C., Luhrmann, R. & Fabrizio, P. The ribosomal translocase homologue Snu114p is involved in unwinding U4/U6 RNA during activation of the spliceosome. *EMBO Rep.* **3**, 875–880 (2002).
- Maeder, C., Kutach, A.K. & Guthrie, C. ATP-dependent unwinding of U4/U6 snRNAs by the Brr2 helicase requires the C terminus of Prp8. *Nat. Struct. Mol. Biol.* **16**, 42–48 (2009).
- Martegani, E. *et al.* Identification of gene encoding a putative RNA-helicase, homologous to SKI2, in chromosome VII of *Saccharomyces cerevisiae*. *Yeast* **13**, 391–397 (1997).
- Xu, D., Nouraini, S., Field, D., Tang, S.J. & Friesen, J.D. An RNA-dependent ATPase associated with U2/U6 snRNAs in pre-mRNA splicing. *Nature* **381**, 709–713 (1996).
- Noble, S.M. & Guthrie, C. Identification of novel genes required for yeast pre-mRNA splicing by means of cold-sensitive mutations. *Genetics* **143**, 67–80 (1996).
- Ponting, C.P. Proteins of the endoplasmic-reticulum-associated degradation pathway: domain detection and function prediction. *Biochem. J.* **351**, 527–535 (2000).
- Holm, L. & Sander, C. Dali: a network tool for protein structure comparison. *Trends Biochem. Sci.* **20**, 478–480 (1995).
- Büttner, K., Nehring, S. & Hopfner, K.P. Structural basis for DNA duplex separation by a superfamily-2 helicase. *Nat. Struct. Mol. Biol.* **14**, 647–652 (2007).
- Richards, J.D. *et al.* Structure of the DNA repair helicase hel308 reveals DNA binding and autoinhibitory domains. *J. Biol. Chem.* **283**, 5118–5126 (2008).
- Rost, B. PHD: predicting one-dimensional protein structure by profile-based neural networks. *Methods Enzymol.* **266**, 525–539 (1996).
- Corpet, F. Multiple sequence alignment with hierarchical clustering. *Nucleic Acids Res.* **16**, 10881–10890 (1988).
- Caruthers, J.M., Johnson, E.R. & McKay, D.B. Crystal structure of yeast initiation factor 4A, a DEAD-box RNA helicase. *Proc. Natl. Acad. Sci. USA* **97**, 13080–13085 (2000).
- Zhao, R., Shen, J., Green, M.R., MacMorris, M. & Blumenthal, T. Crystal structure of UAP56, a DEX/H-box protein involved in pre-mRNA splicing and mRNA export. *Structure* **12**, 1373–1381 (2004).
- Shi, H., Cordin, O., Minder, C.M., Linder, P. & Xu, R.M. Crystal structure of the human ATP-dependent splicing and export factor UAP56. *Proc. Natl. Acad. Sci. USA* **101**, 17628–17633 (2004).
- Sengoku, T., Nureki, O., Nakamura, A., Kobayashi, S. & Yokoyama, S. Structural basis for RNA unwinding by the DEAD-box protein *Drosophila* Vasa. *Cell* **125**, 287–300 (2006).
- Trinh, R., Gurbaxani, B., Morrison, S.L. & Seyfzadeh, M. Optimization of codon pair use within the (GGGS)₃ linker sequence results in enhanced protein expression. *Mol. Immunol.* **40**, 717–722 (2004).
- Boon, K.L. *et al.* PRP8 mutations that cause human retinitis pigmentosa lead to a U5 snRNP maturation defect in yeast. *Nat. Struct. Mol. Biol.* **14**, 1077–1083 (2007).
- Pleiss, J.A., Whitworth, G.B., Bergkessel, M. & Guthrie, C. Transcript specificity in yeast pre-mRNA splicing revealed by mutations in core spliceosomal components. *PLoS Biol.* **5**, e90 (2007).
- Rogers, G.W., Jr., Komar, A.A. & Merrick, W.C. eIF4A: the godfather of the DEAD box helicases. *Prog. Nucleic Acid Res. Mol. Biol.* **72**, 307–331 (2002).
- van Nues, R.W. & Beggs, J.D. Functional contacts with a range of splicing proteins suggest a central role for Brr2p in the dynamic control of the order of events in spliceosomes of *Saccharomyces cerevisiae*. *Genetics* **157**, 1451–1467 (2001).

37. Liu, S., Rauhut, R., Vornlocher, H.P. & Luhrmann, R. The network of protein-protein interactions within the human U4/U6.U5 tri-snRNP. *RNA* **12**, 1418–1430 (2006).
38. Pena, V., Liu, S., Bujnicki, J.M., Luhrmann, R. & Wahl, M.C. Structure of a multipartite protein-protein interaction domain in splicing factor *prp8* and its link to retinitis pigmentosa. *Mol. Cell* **25**, 615–624 (2007).
39. Brenner, T.J. & Guthrie, C. Assembly of Snu114 into U5 snRNP requires Prp8 and a functional GTPase domain. *RNA* **12**, 862–871 (2006).
40. Bartels, C., Urlaub, H., Luhrmann, R. & Fabrizio, P. Mutagenesis suggests several roles of Snu114p in pre-mRNA splicing. *J. Biol. Chem.* **278**, 28324–28334 (2003).
41. Oyama, T. *et al.* Atomic structures and functional implications of the archaeal RecQ-like helicase Hjm. *BMC Struct. Biol.* **9**, 2 (2009).
42. Brow, D.A. & Guthrie, C. Spliceosomal RNA U6 is remarkably conserved from yeast to mammals. *Nature* **334**, 213–218 (1988).
43. Caruthers, J.M. & McKay, D.B. Helicase structure and mechanism. *Curr. Opin. Struct. Biol.* **12**, 123–133 (2002).
44. Häcker, I. *et al.* Localization of Prp8, Brr2, Snu114 and U4/U6 proteins in the yeast tri-snRNP by electron microscopy. *Nat. Struct. Mol. Biol.* **15**, 1206–1212 (2008).
45. Zhang, L. *et al.* Crystal structure of the C-terminal domain of splicing factor Prp8 carrying retinitis pigmentosa mutants. *Protein Sci.* **16**, 1024–1031 (2007).
46. Yang, K., Zhang, L., Xu, T., Heroux, A. & Zhao, R. Crystal structure of the β -finger domain of Prp8 reveals analogy to ribosomal proteins. *Proc. Natl. Acad. Sci. USA* **105**, 13817–13822 (2008).
47. Ritchie, D.B. *et al.* Structural elucidation of a PRP8 core domain from the heart of the spliceosome. *Nat. Struct. Mol. Biol.* **15**, 1199–1205 (2008).
48. Pena, V., Rozov, A., Fabrizio, P., Luhrmann, R. & Wahl, M.C. Structure and function of an RNase H domain at the heart of the spliceosome. *EMBO J.* **27**, 2929–2940 (2008).
49. Rogers, G.W., Jr., Richter, N.J., Lima, W.F. & Merrick, W.C. Modulation of the helicase activity of eIF4A by eIF4B, eIF4H, and eIF4F. *J. Biol. Chem.* **276**, 30914–30922 (2001).
50. Tanaka, N., Aronova, A. & Schwer, B. Ntr1 activates the Prp43 helicase to trigger release of lariat-intron from the spliceosome. *Genes Dev.* **21**, 2312–2325 (2007).
51. Pekkala, M. *et al.* The peptide-substrate-binding domain of collagen prolyl 4-hydroxylases is a tetratricopeptide repeat domain with functional aromatic residues. *J. Biol. Chem.* **279**, 52255–52261 (2004).
52. Chiu, T.K. & Davies, D.R. Structure and function of HIV-1 integrase. *Curr. Top. Med. Chem.* **4**, 965–977 (2004).
53. Colandene, J.D. & Topal, M.D. The domain organization of NaeI endonuclease: separation of binding and catalysis. *Proc. Natl. Acad. Sci. USA* **95**, 3531–3536 (1998).
54. Stutz, F. *et al.* REF, an evolutionary conserved family of hnRNP-like proteins, interacts with TAP/Mex67p and participates in mRNA nuclear export. *RNA* **6**, 638–650 (2000).
55. Jermy, A.J., Willer, M., Davis, E., Wilkinson, B.M. & Stirling, C.J. The Brl domain in Sec63p is required for assembly of functional endoplasmic reticulum translocons. *J. Biol. Chem.* **281**, 7899–7906 (2006).

ONLINE METHODS

Yeast strain and plasmids. We generated the *brr2-3GS*, *brr2-1* and R1107A mutations on the pGPD-Brr2-TAP vector¹⁸ (gift of S. Stevens) using the QuikChange Site-Directed Mutagenesis Kit (Stratagene) and confirmed all mutations by DNA sequencing of the entire Brr2 coding region. The mutated plasmid was shuffled into pTB105 and its growth phenotype was compared to the strain containing wild-type *Brr2* on the same plasmid in pTB105. We generated Brr2-deletion constructs on pPR150 (ref. 11) by amplifying the pPR150 plasmid without the deletion region, using PCR primers containing a common restriction site for subsequent digestion and ligation. A similar strategy was used to generate the S2-deleted *brr2* on the pGPD-Brr2-TAP vector. The wild-type and truncated pPR150 plasmids were shuffled into yeast strain yJPS996 (ref. 13; gift of J. Staley) for growth phenotype or pull-down analyses.

Protein expression and purification. We subcloned the Brr2 S2 domain into the pGEX-6p1 vector (GE Healthcare) and expressed it in *Escherichia coli* strain XA90 as a GST-fusion protein. The fusion protein was first purified using glutathione Sepharose resin and cleaved using PreScission protease. The resultant S2 domain was further purified on a Superdex-200 (S200) gel filtration column (GE Healthcare) and concentrated to 10 mg ml⁻¹ for crystallization trials. Selenomethionine (SeMet)-substituted S2 domain was expressed in minimal medium containing SeMet. The protein was then purified using glutathione resin, then a Resource Q column (GE Healthcare), followed by the S200 column. The purified protein was concentrated to 12 mg ml⁻¹ for crystallization trials.

The Brr2 H2 and H2+S2 domains used for RNA binding experiments and the hemagglutinin (HA)-tagged H2, S2 and H2+S2 domains used for GST pull-down experiments were also subcloned into the pGEX-6p1 vector, and expressed and purified similarly to the S2 domain. The GST-fused Brr2, Prp8 and Snu114 proteins used in GST-pull down experiments were obtained similarly, without the PreScission cleavage and gel filtration purification.

Wild-type and mutated Brr2 were expressed in yeast strain yTB105 containing the pGPD-BRR2-TAP or pGPD-BRR2-mutant-TAP plasmid and purified as described¹⁸, with the following exceptions. The frozen cell paste was homogenized with a SPEX SamplePrep 6870 Freezer Mill. The proteins were cleaved off the IgG resin using TEV protease and dialyzed into the storage buffer (20 mM HEPES, pH 7.9, 100 mM NaCl, 5 mM β-mercaptoethanol, 0.2 mM EDTA, 0.01% (v/v) NP40, 20% (v/v) glycerol) for subsequent enzymatic and EMSA analyses.

Crystallization, data collection and structure determination. We crystallized the Brr2 S2 domain by the hanging drop vapor diffusion method using a well solution containing 0.1 M sodium citrate, pH 6.0, 17% (w/v) PEG8000 and 0.2 M NaCl. All crystallographic data were collected at 100 K using the Molecular Biology Consortium beamline 4.2.2 of the Advanced Light Source at Lawrence Berkeley National Laboratory. Data were processed using the d*trek package⁵⁶, and data statistics are shown in **Table 1**.

We determined the structure of S2 using the SeMet MAD method and the programs Solve and Resolve⁵⁷. Model building was carried out using O⁵⁸. Refinement was performed using CNS⁵⁹ and the peak data set. Refinement statistics are shown in **Table 1**. 90.2% and 9.8% of the residues fall into the most favored and additionally allowed regions, and no residues are in the generously allowed and disallowed regions of the Ramachandran plot.

ATPase and helicase assays. We performed ATPase and helicase assays as described¹⁸, 250 nM Brr2 proteins and 1 μM U4/U6 used in ATPase assays and 25 nM Brr2, 250 nM Prp8-CTR and 200 nM U4/U6 in helicase assays.

Splicing microarray. To monitor pre-mRNA splicing defects on a global scale, we carried out whole-genome splicing microarrays analyses as described⁶⁰. Samples for both the *brr2-S2del* strain and its matched wild-type strain were collected at 30 °C for splicing microarray analyses. Samples for the *brr2-1* strain and its matched wild type were collected after shifting to 16 °C for 10 min.

Quantitative reverse-transcription-polymerase chain reaction. We performed quantitative RT-PCR as described⁶⁰, using a Roche LightCycler 480 and the following primers: U1: forward (F), 5'-TGACTACTTTTCTC TAGCGTGCC-3'; reverse (R), CATAACGGGAACGAGCAAAGTTG-3'. U2: F, 5'- AACTGAAATGACCTCAATGAGGCTC-3'; R, 5'-AGACCTGACATTAGCG GAAAACAAC-3'. U4: F, 5'- ATCCTTATGCACGGAAATACG-3'; R, 5'- AAAG GTATTCCAAAATTCCTAC-3'. U5: F, 5'- CAAGCAGCTTTACAGATCAAT

GG-3'; R, 5'-AGTTCCAAAAAATATGGCAAGCC-3'. U6: F, 5'- GTTCGCGA AGTAACCCCTTCG-3'; R, 5'- AAAACGAAATAAATCTCTTTGTAAAC-3'. YMR286w: F, 5'-GTTGAGTAGGTCGCTTATCGGTGT-3'; R, 5'- CTTTACTT TAGCTAGGAGCCAGC-3'. YAL010c: F, 5'- ATAGCTACGAGGATATAACGGC CA-3'; R, 5'- AATTGCTGTGCATCGGAGTATAAAT-3'. Sample loading was normalized according to the composite behavior of the YMR286w and YAL010c genes.

Protein and RNA interaction using electrophoresis mobility shift assay. We ordered short 13-nt RNA oligonucleotides (ssR13 and its complementary sequence) from Integrated DNA Technologies. We labeled ssR13 on its 5' end with ³²P-γ-ATP using Optikinase (USB Corporation). We generated dsR13 by combining labeled ssR13 and its complementary sequence, boiling for 3 min and cooling to room temperature (22 °C) in about 3 h. U4 was *in vitro* transcribed from pT7U4 linearized with Sty1 using T7 RNA polymerase and in the presence of α-³²P-UTP⁶¹. U6 was transcribed from pT7U6Δ(U) (first two uracils removed from U6 to increase transcription efficiency) linearized with Dra1 (ref. 8). Both RNAs were purified by extraction from a 6% (w/v) urea-TBE denaturing polyacrylamide gel, phenol-chloroform extraction and ethanol precipitation. The U4/U6 duplex was generated by combining U4 and U6 RNAs in 40 mM Tris-HCl, pH 7.4, and 100 mM sodium acetate, boiling for 3 min and cooling to room temperature in about 3 h.

RNA was incubated on ice with protein (UAP56, Prp8-CTR and various Brr2 proteins) in 20 μl of 10 mM HEPES, pH 7.6, 1 mM MgCl₂, 100 mM NaCl, 5% (v/v) glycerol, and in the absence or presence of 1 mM ATP, for 60 min. In supershift experiments, anti-Brr2 or anti-Prp8 antibody was added in the binding reaction after 30 min and was incubated for another 30 min on ice. The reaction mixture was separated on a 4% native polyacrylamide gel in TBE buffer (for short 13-nt RNAs) or HEPES buffer (20 mM HEPES, pH 7.9, for U4/U6), visualized and quantified using a phosphorimager.

GST-pull down experiments. GST-fused Snu114, Brr2 and Prp8 fragments were incubated with glutathione resin at 4 °C for 2 h in the binding buffer (50 mM Tris-HCl, pH 7.5, 120 mM NaCl, 0.2% (v/v) NP40, 10% (v/v) glycerol, 2 mM EDTA, 1 mM DTT, 1 mg ml⁻¹ BSA) and washed three times with the wash buffer (50 mM Tris-HCl, pH 8, 100 mM NaCl, 0.5% (v/v) NP40, and 1 mM EDTA). Resin carrying equal quantities of fusion protein were incubated with HA-tagged Brr2 domains (H2, S2 or H2+S2) at 4 °C for 2 h. The resin was washed four times with low-salt buffer (50 mM Tris-HCl, pH 7.5, 120 mM NaCl, 0.2% (v/v) NP40, 10% (v/v) glycerol, 2 mM EDTA, 1 mM DTT) and three more times with high-salt buffer (same as the low-salt buffer but containing 500 mM NaCl and 0.5% (v/v) NP40). The resin was then analyzed using western blot with an anti-HA antibody.

Co-immunoprecipitation. Yeast strains were grown to an optical density at 600 nm (OD₆₀₀) of 1.0. Cells with an OD₆₀₀ of 20 were harvested by centrifugation, washed with 1 ml of buffer A (10 mM HEPES, pH 7.9, 100 mM NaCl, 5 mM benzimidazole, 2 mM PMSE, 5 mM N-ethylmaleimide, 2 mM EDTA), and resuspended in 200 μl of buffer B (0.1% deoxycholic acid, 1 mM EDTA, 50 mM HEPES-KOH, pH 7.5, 140 mM NaCl, 1% (w/v) Triton X-100, 1 mM PMSE, 1× protease inhibitors cocktail (Roche)). Cells were lysed using the bead beater and separated using centrifugation. The supernatant containing 1.6 mg of total protein was incubated with 5 μl anti-polyoma antibody (Covance) overnight at 4 °C. We then added 30 μl protein G agarose (GE Healthcare) to the mixture and incubated it at 4 °C for 2 h. The resin was washed four times with buffer B. The resin was then run on a 6% SDS-PAGE gel and analyzed using western blotting with specific antibodies.

- Pflugrath, J.W. The finer things in X-ray diffraction data collection. *Acta Crystallogr. D Biol. Crystallogr.* **55**, 1718–1725 (1999).
- Terwilliger, T.C. & Berendzen, J. Automated MAD and MIR structure solution. *Acta Crystallogr. D Biol. Crystallogr.* **55**, 849–861 (1999).
- Jones, T.A., Zou, J.Y., Cowan, S.W. & Kjeldgaard, M. Improved methods for building protein models in electron density maps and the location of errors in these models. *Acta Crystallogr. A* **47**, 110–119 (1991).
- Häcker, A.T. *et al.* Crystallography & NMR system: a new software suite for macromolecular structure determination. *Acta Crystallogr. D Biol. Crystallogr.* **54**, 905–921 (1998).
- Inada, M. & Pleiss, J.A. Genome-wide approaches to monitor pre-mRNA splicing. in *Methods Enzymol.* (in the press).
- Salghetti, S.E., Kim, S.Y. & Tansey, W.P. Destruction of Myc by ubiquitin-mediated proteolysis: cancer-associated and transforming mutations stabilize Myc. *EMBO J.* **18**, 717–726 (1999).